

***Cy-mag*<sup>3D</sup>: a simple and miniature climbing robot with advance mobility in ferromagnetic environment**

FREDERIC ROCHAT\*, PATRICK SCHOENEICH, BARTHELEMY LUTHI,  
FRANCESCO MONDADA, HANNES BLEULER

*Laboratoire de Systèmes Robotiques (LSRO), Mobots group,  
Ecole Polytechnique Fédérale de Lausanne (EPFL),  
Lausanne, 1015, Switzerland  
E-mail: frederic.rochat@epfl.ch  
<http://mobots.epfl.ch>*

ROLAND MOSER

*Inspection Technologies,  
ALSTOM Power,  
Baden, Switzerland*

*Cy-mag*<sup>3D</sup> is a miniature climbing robot with advanced mobility and magnetic adhesion. It is very compact: a cylindrical shape with 28 mm of diameter and 62 mm of width. Its design is very simple: two wheels, hence two degrees of freedom, and an advanced magnetic circuit. Despite its simplicity, *Cy-mag*<sup>3D</sup> has an amazing mobility on ferromagnetic sheets. From an horizontal sheet, it can make transition to almost any intersecting sheet from 10° to 360° – we baptise the last one surface flip. It passes inner and outer straight corners in any almost inclination of the gravity. *Cy-mag*<sup>3D</sup> opens new possibilities to use mobile robots for industrial inspection with stringent size limitations, as found in generators. A patent is pending on this system.

*Keywords:* robot, mobile, miniature, wheel, climbing, magnetic adhesion

## 1. Introduction

Industry requires robotic solutions to inspect power plants. We focus on 3D mobility to inspect ferromagnetic environment with stringent size limitation in generators. In ferromagnetic environment magnetic adhesion is a straightforward choice.<sup>1</sup> Existing robots passing obstacles using wheels<sup>2</sup> and caterpillars<sup>3</sup> show very good performances. In this paper, we present *Cy-mag*<sup>3D</sup> (Fig. 1), our miniature robot which is able to climb on ferromagnetic surfaces regardless of the direction of the gravity. Thanks to its



Fig. 1. *Cy-mag<sup>3D</sup>*: ferromagnetic miniature climbing robot with cylindrical shape

innovative design the robot achieves superior mobility than more complex and larger previous designs. The robot can be described as a magnetic *Segway*,<sup>4</sup> where the gravity force is replaced by a magnetic force. Since the magnetic force is acting below the axis of rotation, the system is stable and thus does not need advanced control. The cylindrical shape allows excellent mobility, robustness and compactness, similar to the all-terrain scout robot for example.<sup>5</sup>

## 2. Mobility

The mobility innovation of the robot is that the holding torque — preventing the cylinder to move freely — is magnetic. When the motors activate the wheels forward, the body is hold by the magnetic torque and the robot moves forward until it encounters an obstacle. When the robot is in front of an obstacle — as an inner plan transition for example — the body rotates backward, commuting the magnetic adhesion from one surface to the other. Fig. 2a shows the inner angle passage steps. With this robot and its novel magnetic configuration, the problem of the wheel blocked in the corner is removed.<sup>6,7</sup> The robot can move on flat non magnetic surfaces. Due to its cylindrical shape the robot can easily recover in case it would fall off on its “roof”.

### 2.1. Magnetic design

We design a magnetic circuit that creates a sufficient holding torque for forward movement and facilitates adhesion commutation in obstacle passing phase. The magnetic design is started by an analytical computation of the force generated by a simplified magnetic circuit. It is composed by

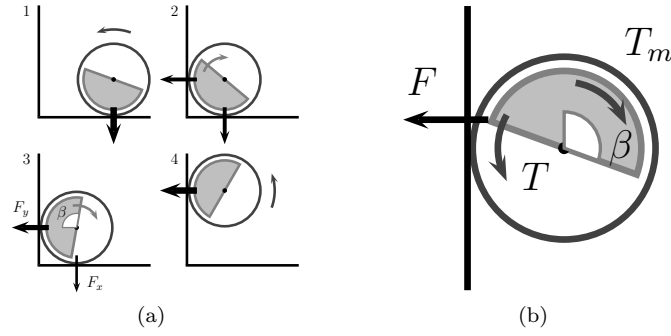


Fig. 2. (a): Passage phases of an inner straight angle regardless of the gravity. When the wheels cannot rotate forward due to an obstacle, the magnetic circuit rotates backwards and thus transfer the adhesion force to the new surface. When the transfer is finished, the holding force is sufficient to move on the new surface. (b): Magnetic force  $F$ , magnetic holding torque  $T$  and motor torque  $T_m$  on the robot structure.

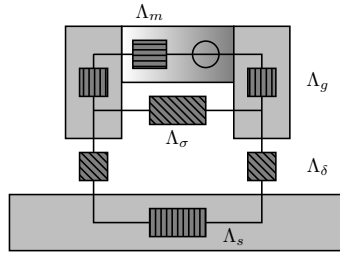


Fig. 3. Magnetic model of the system. The stripped boxes show the permeances  $\Lambda$  of all different sub-parts (m: magnet, g: flux guide, s: surface,  $\delta$ : airgap,  $\sigma$ : leakage).

a cylindrical magnet encompassed with two iron flux guides. A compact design is sought. Calculations will give a first estimation of the system dimension. The equivalent model is shown in Fig. 3 and the computations are shown in the next chapter.

### 2.2. Analytical computations

We consider a cylindrical magnet, with steel flux guides on the sides (Fig. 3). The worst case arise during flips from one side of a plate to the other side. Thus we take a  $2mm$  sheet and design our magnetic system to hold in this worst case.

The permeance of the flux guides is considered as infinite. The external permeance  $\Lambda_e$  (Equ. 2) is the sum of the airgap permeance  $\Lambda_\delta$ , the surface

permeance  $\Lambda_s$ , and of the leakage permeance  $\Lambda_\sigma$  (Equ. 1). For the following,  $l_\alpha$  will represent the corresponding length of each part  $\alpha$ , and  $S_\alpha$  will represent its cross section.

$$\Lambda_\delta = \frac{\mu_0 S_\delta}{2\delta}, \Lambda_\sigma = \frac{\mu_0 S_\sigma}{l_\sigma}, \Lambda_s = \frac{\mu_0 S_s}{l_s} \quad (1)$$

$$\Lambda_{\delta+s} = \frac{1}{\frac{1}{\Lambda_\delta} + \frac{1}{\Lambda_s}}, \Lambda_e = \Lambda_{\delta+s} + \Lambda_\sigma \quad (2)$$

The load line slope  $K$  of the magnet is then computed (Equ. 3).

$$K = \Lambda_e \frac{l_m}{S_m} \quad (3)$$

The final induction in the magnet  $B_m$  (Equ. 5) is the intersection of the magnet B-H curve with the load line (Equ. 4).

$$B_m = B_r + \mu_m \mu_0 H_m = -K H_m \quad (4)$$

$$B_m = \frac{B_r}{1 + \frac{\mu_m \mu_0}{K}} \quad (5)$$

$B_r$  being the residual induction of the magnet,  $\mu_m$  its relative permeability, and  $H_m$  the coercive force.

The flux is dividing in two parts and pass through  $\Lambda_\delta$  and  $\Lambda_\sigma$ . Thus the induction in the airgap is computed and shown in Equ. 6.

$$B_\delta = B_m \frac{S_m}{S_\delta} \frac{\Lambda_{\delta+s}}{\Lambda_{\delta+s} + \Lambda_\sigma} \quad (6)$$

Finally the attracting force  $F$  is shown in Equ. 7.

$$F = \frac{B_\delta^2 S_\delta}{2\mu_0} \quad (7)$$

Using  $B_r = 1.27$  T,  $\mu_m = 1.05$  [-],  $\delta = 1$  mm,  $S_\delta = 6 \times 2$  mm<sup>2</sup>,  $l_m = 40$  mm,  $S_m = \pi \times 4.9^2$  mm<sup>2</sup>,  $S_\sigma = 300$  mm<sup>2</sup>,  $l_\sigma = 40$  mm,  $S_s = 100$  mm<sup>2</sup> and  $l_s = 40$  mm, we obtain an adhesion force  $F$  of 7.2 N. Thus such a system can theoretically hold 720 g.

### 2.3. Magnetic simulations

3D simulations of the magnetic system have been done using the software *Comsol*. Forces and torque acting on the system in different conditions can

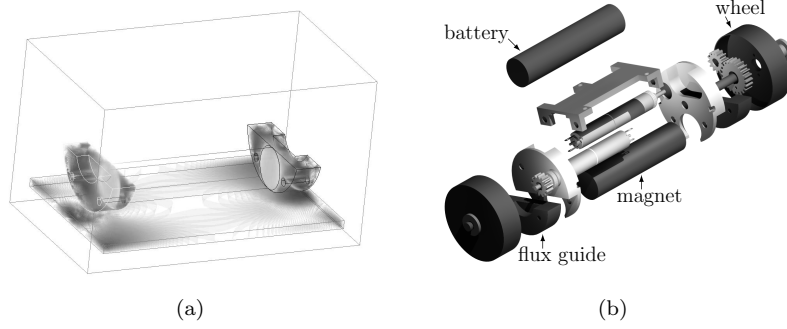


Fig. 4. (a): 3D magnetic simulation of the built system on a plate, the magnetization is shown. (b): Exploded view of the robot.

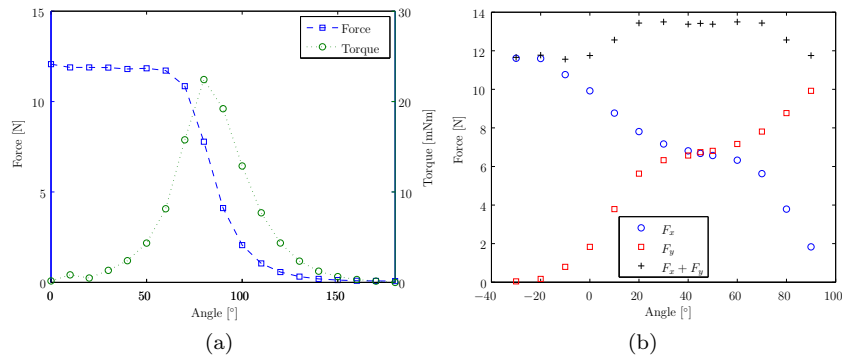


Fig. 5. (a) Simulation of the magnetic force and torque of the magnetic system rotating around its axis on a plate (as shown in Fig. 2b) and (b) Simulation of the magnetic forces  $F_x$  and  $F_y$  on each surfaces during an inner plan transition (as shown in Fig. 2a). We can see that the total holding force is never going down, and thus the robot is stable during all the process.

be computed. Fig. 5a shows the force and torque applied to the magnetic system rotating around the axis of the robot on a plate. An important point here is the maximum torque: it must be big enough to maintain the robot when going up. Fig. 5b shows the force evolution on the first and second plate during an inner plan transition. We can see that the total force never decreases, and thus the robot is always secure.

#### 2.4. *Magnetic force measures*

Measures have been done using an experimental setup with a dynamometer to confirm the magnetic system capabilities. The obtained holding force is  $7.9\text{ N}$ . The computed and simulated adhesion forces are thus validated. As the robot weighs  $83\text{ g}$  we have more than enough force and thus a very good safety coefficient, which is useful in some perilous situation.

The maximum torque on the system has also been measured. This value is important to ensure that the robot does not fall back when going upwards a wall (see Fig. 2b). The obtained value is of  $15\text{ mNm}$ . The inner corner maximal transition torque has also been measured. It is important for it to be low so that the robot will not get stuck. Its value is of  $6\text{ mNm}$ . Compared to the torque of  $11\text{ mNm}$  needed to climb up on a vertical surfaces, those values show that the robot using this magnetic arrangement will work as expected.

### 3. Robot realization

The robot weighs  $83\text{ g}$ , thus the torque needed to go uphill (obtained by multiplying the weight by the radius) is of  $11\text{ mNm}$ . Two  $6\text{ mm}$  diameter Maxon motors with 221:1 gearboxes are chosen. They deliver a sufficient continuous torque of  $72\text{ mNm}$  each. An aluminium frame is holding both wheels, the motors, the magnetic circuit and the electronics. Two gears are used for each wheel to shift the rotation axis of the motor from the one of the wheels (Fig. 4b).

The robot embeds a dsPic microcontroller. It allows to control the motors and to receive commands from the user by infrared. Two distance sensors can guide alignment of the robot in front of walls. A lithium-ion battery stores the energy. It has a capacity of  $500\text{ mAh}$  and its autonomy is close to 1 hour.

### 4. Results

The robot operates as expected. It is able to move on ferromagnetic surfaces in any orientation, and pass almost every possible edge. It can pass all inner corners with angles' value from  $10$  to  $180^\circ$  in any orientation (see Fig. 6). All outer corners are also possible, but care has to be taken when the robot is going down after the transition, as the robot passes from one equilibrium position to the other one, and thus makes a fast forward movement which is uncontrolled and might result in detaching the robot (shown as  $\triangle^a$  on the figure). Insufficient friction reduces the chances of passing some outer

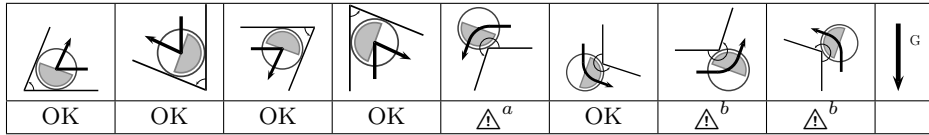


Fig. 6. Edges' transitions in different orientations for acute and obtuse angles (10 to 300°).

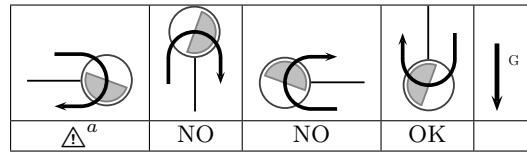


Fig. 7. Surface flips in different orientations of gravity.

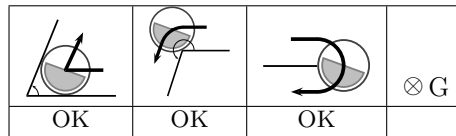


Fig. 8. Transitions with lateral gravity.

corners depending on the orientation of gravity and their sharpness (shown as  $\Delta^b$  on the figures).

Flips from one side to the other of a plate are also possible in some cases (Fig. 7). Mobility with gravity along the length axis of the robot shows the best performances as there are no stability problems (Fig. 8). As the robot is robust, it can easily recover from falls. Experiences showed that 40 cm is not a problem. Due to its cylindrical shape the robot never gets stuck and can continue its mission.

### 5. Conclusion

We invented, designed, prototyped and tested a miniature ferromagnetic climbing robot –  $\varnothing 28\text{ mm} \times 62\text{ mm}$  – named *Cy-mag<sup>3D</sup>*. The robot locomotion is based on a patented innovative idea, which confers compactness, simplicity, robustness and high mobility on it. The robot can pass acute angle and surface flips that no other robot can pass in those dimensions. It can pass straight inner corners in all inclination as some outer straight edges. Ongoing work exploits the patented idea in other configurations. Additionally, new prototypes will embed vision. The simplicity, mobility

and miniaturization of this robot opens new avenues for industrial robotics inspection.

## 6. Acknowledgment

This project was founded by the Swiss CTI project: *Highly compact robots for power plants inspections* referenced as CTI 8435.1 EPRP-IW and *Alstom*. We are thankful to Pierre Noirat, Tarek Baaboura and André Guignard for their uncountable manufacturing skills and talents. We also want to thank Daniel Burnier, Phillipe Rétornaz, Stéphane Magnenat and Michael Bonani for their support for electronics and software.

## References

1. D. Longo and G. Muscato, Adhesion techniques for climbing robots stat of the art and experimental consideration, in *Climbing And Walking Robots: Proceedings of the 11th International Conference on Climbing and Walking Robots and the Support Technologies for Mobile Machines (CLAWAR 2008)*, (Coimbra, 2008). 4.
2. F. Tâche, W. Fischer, R. Siegwart, R. Moser and F. Mondada, Compact magnetic wheeled robot with high mobility for inspecting complex shaped pipe structures, in *IEEE/RSJ International Conference on Intelligent Robots and Systems (IROS 2007)*, 2007. 5.
3. F. Rochat, P. Schoeneich, O. T.-D. Nguyen and F. Mondada, Tripillar: Miniature magnetic caterpillar climbing robot with plane transition ability, in *CLAWAR 2009*, eds. O. Tosun, H. L. Akin, M. O. Tokhi and G. S. Virk, Proceedings of 12th International conference on climbing and walking robots and the support technologies for mobile machines (CLAWAR), Vol. 1 (Istanbul, 2009).
4. H. Nguyen, J. Morrell, K. Mullens, A. Burmeister, S. Miles, N. Farrington, K. Thomas and D. Gage, *SPIE Mobile Robots XVII* (2004).
5. A. Drenner, I. Burt, B. Kratochvil, B. J. Nelson, N. Papanikolopoulos and K. B. Yesom, Communication and mobility enhancements to the scout robot, in *IEEE/RSJ International Conference on Intelligent Robots and System*, 2002. 5.
6. F. Tâche, W. Fischer, R. Moser, F. Mondada and R. Siegwart, Adapted magnetic wheel unit for compact robots inspecting complex shaped pipe structures, in *Proceedings of the 2007 IEEE/ASME International Conference*, 2007. 4.
7. Y. Kawaguchi, I. Yoshida, H. Kurumatani, T. Kikuta, Y. Yamada and O. Ltd, *Proceedings of the IEEE International Conference on Robotics and Automation* 1 (1995).